ISSUE: March 2014

The Small-Signal Model Of An Active-Clamp Forward Converter (Part 2): Active-Clamp Forward Converter Operation

by Christophe Basso, ON Semiconductor, Toulouse, France

The first part of this series was dedicated to the study of the classical tertiary winding-based forward converter. In the forward topology, energy is absorbed from the source and transmitted to the load during the power switch on-time. During this period, the magnetizing current energizes the core but plays no role in the power transfer. To keep the core away from saturation, you must ensure a proper demagnetization of the transformer before the next cycle takes place. This is the goal of the tertiary winding with its voltage stress and hard switching drawbacks.

The active-clamp technique not only limits the voltage excursion on the power transistor drain at turn-off, it also helps achieve near-zero voltage switching (ZVS) operation under certain conditions. When switching losses are minimized, it becomes easier to increase the switching frequency and reduce the size of the magnetics. Here in part 2 of this article series, the structure of the active-clamp forward converter is introduced, its operation is explained, and a large-signal model is derived, enabling SPICE simulation of the converter and generation of its Bode plot. These steps will set the stage for derivation of a small-signal model and a complete control-to-output transfer function for the active-clamp converter in part 3.

The Forward Converter With Active Clamp

A simplified forward converter with the active clamp appears in Fig. 1. Going from the classical forward converter to this active-clamp variation, we see that the secondary side does not change, it is still a buck-derived topology. What changes is the primary side where the transformer no longer features a tertiary winding. Another controlled switch, Q_2, has appeared, connecting the drain node to an extra capacitor C_{clp}.

In this representation, C_{clp} is connected to the dc input line through an n-channel transistor, Q_2, whose body diode is purposely drawn. This transistor requires a special high-side driver as its source floats. This driver can be in the form of a dedicated integrated circuit but a high-voltage pulse transformer will do as well.

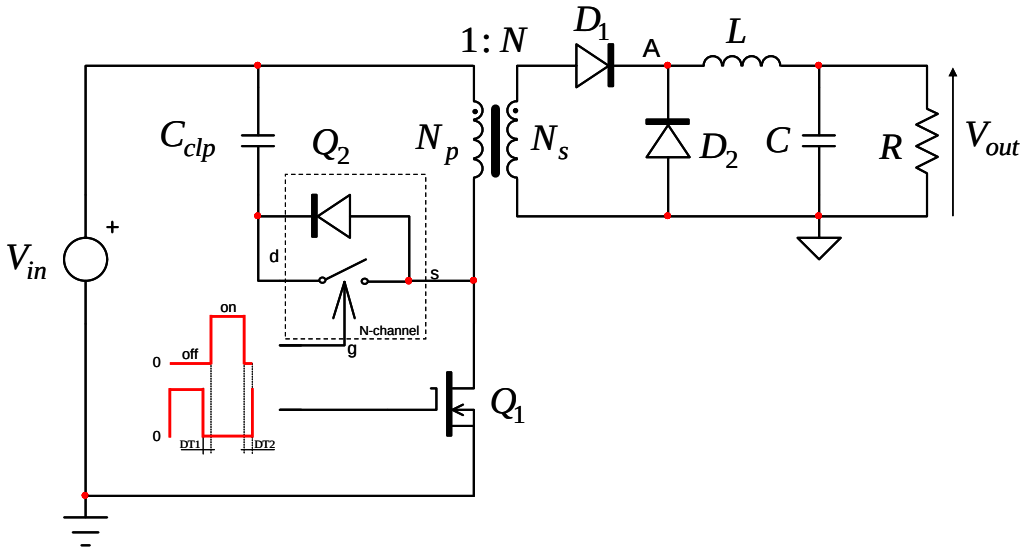

Fig. 1. The clamp capacitor, C_{clp}, is connected to the input dc rail and limits the drain voltage excursion of Q_1 at turn off.

While n-channel transistors are commonly implemented in offline (90- to 265-V ac input) ac-dc active clamp converters (which see up to 400 V on the dc rail), most dc-dc telecom bricks (which feature a lower input

voltage of 36 V to 72 V) adopt a p-channel transistor. As represented in Fig. 2 the clamp capacitor is now referenced to ground, allowing the usage of a p-channel transistor whose ground-referenced driving voltage is simpler to generate than the floating drive signal in the previous solution. Intuitively, if the drain stress is similar in both configurations for Q_1, the voltage rating for C_{clp} in the p-channel option is larger than that with the n-channel.

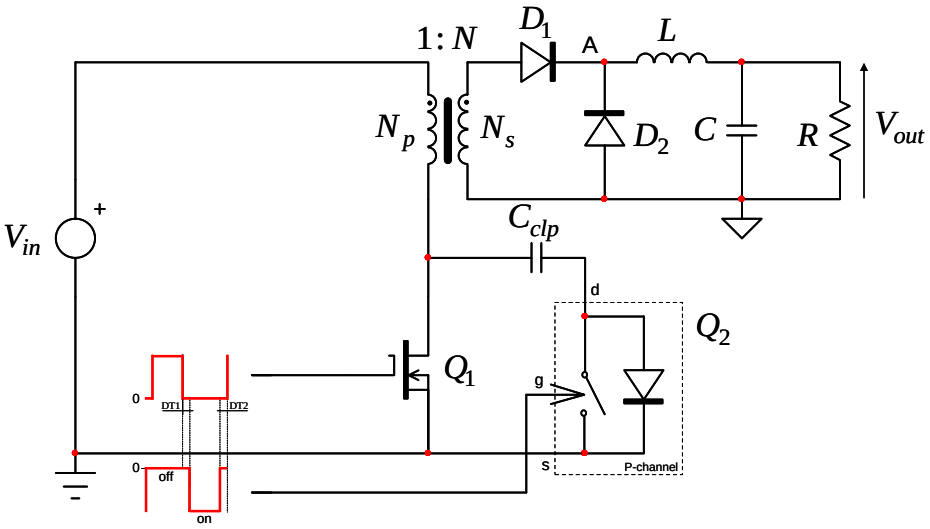

Fig. 2. The clamp capacitor can also be connected to ground via a p-channel MOSFET.

Basics Of Operation

The goal in this section is to provide a brief explanation of how an active-clamp forward converter operates with the adoption of the reset scheme introduced in Fig. 1. This is not meant to be an exhaustive study of the converter's intricacies. For readers interested in more information along those lines, please refer to the references at the end of this article.

Everything starts with the power switch closure. The equivalent circuit at turn-on appears in Fig. 3. It is similar to the classical forward operation. The voltage applied to the magnetizing inductance during turn-on depends on the voltage drop across Q_1:

$$v_{mag}(t) = V_{in} - v_{loss}(t) \quad (1)$$

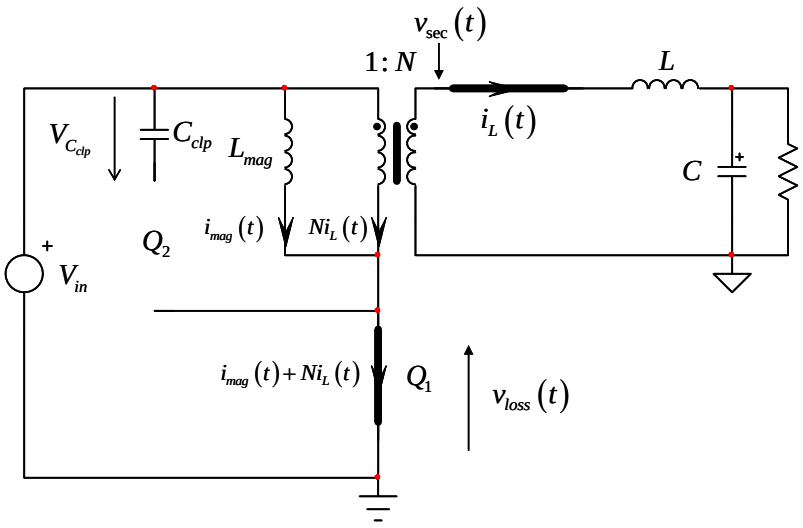

Fig. 3. At turn-on, the drain node is grounded: magnetizing current builds up in the core.

The current circulating in the MOSFET at that time is made of the reflected inductor current $i_L(t)$ and the magnetizing current $i_{mag}(t)$. The MOSFET instantaneous loss is simply:

$$v_{loss}(t) = i_D(t) r_{on1} = \left[i_{mag}(t) + Ni_L(t) \right] r_{on1}. \quad (2)$$

At the end of the on-time, the magnetizing current I_{mag} has reached a value expressed as

$$I_{mag,peak} = S_{mag} t_{on} \quad (3)$$

in which the primary-side slope S_{mag} can be expressed as

$$S_{mag} = \frac{V_{mag}}{L_{mag}} \approx \frac{V_{in}}{L_{mag}}. \quad (4)$$

On the secondary side, the primary-side voltage defined by equation 1 is scaled by the transformer turns ratio N and drives the power inductor L:

$$v_{sec}(t) = N\left(V_{in} - \left[i_{mag}(t) + Ni_L(t) \right] r_{on1} \right). \quad (5)$$

Please note the contribution of the instantaneous loss via the power switch $r_{DS(on)}$, which is denoted as r_{on1} in the above and subsequent equations. This is the important thing about the active-clamp structure: the magnetizing current circulating on the primary side must be accounted for during the analysis, otherwise the power stage ac response remains that of the classical forward.

When the switch opens, the current keeps circulating in the same direction and finds a path through the lumped capacitance C_{lump} offered by the drain node. This capacitance is actually composed of various parasitic elements such as the transformer capacitance and the MOSFET stray elements, C_{oss} and C_{rss}. With the opening of the switch, the schematic updates to that of Fig. 4. The voltage on the drain quickly increases at a pace depending on C_{lump} and $I_{mag,peak}$.

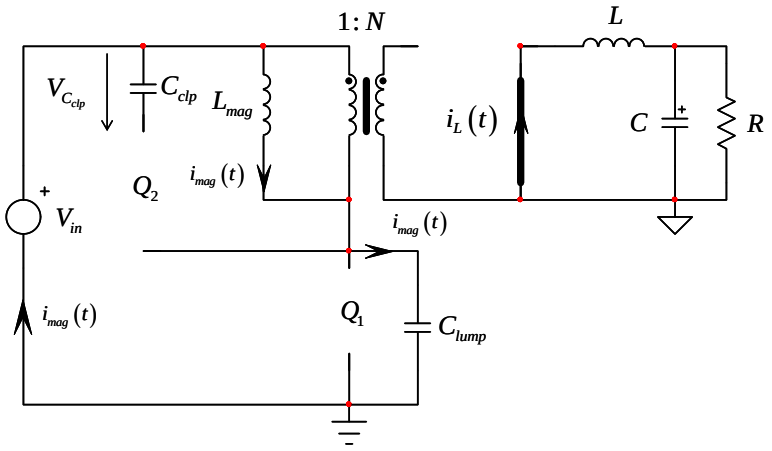

Fig. 4. At turn-off, the magnetizing current charges the lumped capacitance present on the drain and $v_{DS}(t)$ increases quickly.

When the value of the drain voltage crosses V_{in}, the secondary-side diode D_1 commences to block and the output inductor current $i_L(t)$ transfers to the freewheeling diode D_2: the reflected current $Ni_L(t)$ disappears from the primary side and $i_{mag}(t)$ alone keeps circulating. The current transition from D_1 to D_2 during which both diodes simultaneously conduct (the so-called overlap) lasts a small amount of time. Now $v_{DS}(t)$ continues its excursion until it hits the clamp capacitor voltage. At that point, the Q_2 body diode spontaneously conducts and the current now circulates in a closed circuit like that represented in Fig. 5.

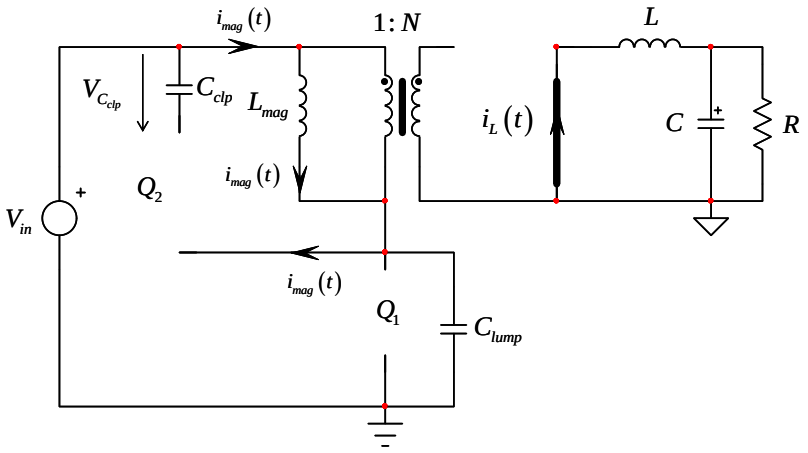

Fig. 5. When the drain voltage hits the clamp level, the Q_2 body diode starts to conduct and the magnetizing current circulates in C_{clp}.

Shortly after this event—the first dead-time duration—the controller instructs Q_2 to turn on. As it happens while its V_{DS} is almost 0 V (the body diode conducts), so ZVS operation is ensured. The power switch drain terminal is clamped to

$$V_{clamp}(t) = V_{in} + V_{clp}(t) + r_{on2} i_{mag}(t). \quad (6)$$

The voltage across the magnetizing inductance has reversed and its current starts to decline with a slope equal to

$$S_{mag} \approx -\frac{V_{clp}}{L_{mag}} \tag{7}$$

given a constant clamp-capacitor voltage. In reality, the voltage on the clamp capacitor slightly increases and peaks to a value obtained when $i_{mag}(t) = 0$. At this moment, the transformer core is reset. Now that the current is 0 A, it changes direction since Q_2 is still closed. The magnetizing current circulates backwards, still in a closed circuit as shown in Fig. 6. It now increases negatively and reaches another peak at which the energy stored in the magnetizing inductor is:

$$E_{mag} = \frac{1}{2} L_{mag} I_{mag,peak}{}^2. \tag{8}$$

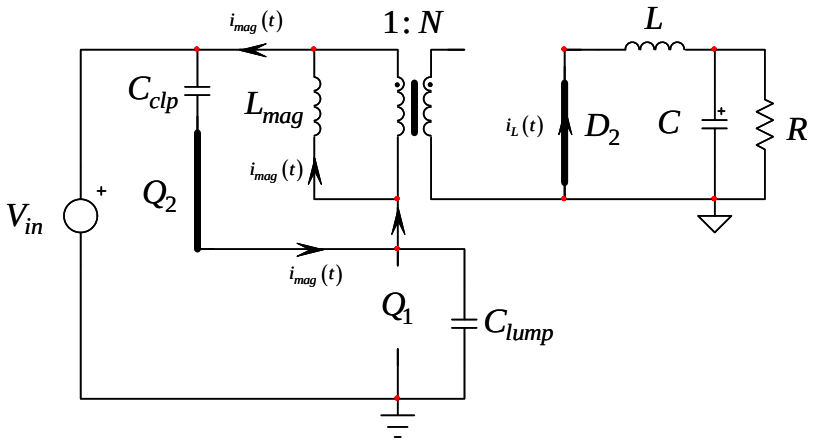

Fig. 6. The magnetizing current has reached 0 A and Q_2 body diode has stopped conducting. However, Q_2 is still closed and the current reverses.

Next, the controller instructs Q_2 to open, forcing the magnetizing current to adopt another circulating path. The current now goes through the input source and returns via the Q_1 parasitic capacitance C_{lump}: this capacitor now resonates with the magnetizing inductance and starts to discharge (Fig. 7.). The drain voltage decreases from the clamp voltage equal to V_{in} + V_{clp} down to the input voltage V_{in}. At this moment—separated from the instant Q_2 was turned off by the second dead time DT2—the controller switches Q_1 on again and another cycle takes place. Because the drain-source voltage has been reduced, switching losses are greatly diminished. Equation 8 is important because it corresponds to the available energy stored in the magnetizing inductance when Q_2 opens. It is this energy that will be used to discharge C_{lump}.

When the drain is at V_{in} and wants to go further down, the secondary-side diode starts to conduct again and the inductor current $i_L(t)$ now reflects to the primary side, scaled by the transformer turns ratio N. By doing so, it opposes the magnetizing current and hampers the C_{lump} discharge process. To ensure a stronger discharge, you need to widen the transformer's air gap in order to reduce L_{mag} and boost the magnetizing current. However, at some point, the circulation of this current would create unacceptable losses on the primary side. Remember, this current does not contribute to the primary-to-secondary energy transfer but it contributes to losses in Q_1 now that it is has been increased significantly for active-clamp purposes.

For this reason, designers usually accept a reduction of the drain-source voltage down to V_{in} at full power and when the output dc current reduces (under light to no-load conditions), so almost full ZVS can be attained.

Typical simulated operating waveforms where the converter is at equilibrium appear in Figs. 8 and 9. At the power switch opening, the drain-source voltage reaches the clamp voltage via the spontaneous conduction of the Q_2 body diode. Q_2 is turned on several tens of nanoseconds later and ZVS is ensured (DT1 duration). The drain voltage is nicely clamped to an almost constant level, V_{clamp}. This level resonates and reaches its maximum when the magnetizing current is 0 A. The magnetizing current then increases in the other direction and reaches another negative peak. The controller instructs the active clamp switch Q_2 to open and the magnetizing current discharges the lumped capacitor. After DT2, the power switch Q_1 is reactivated and switching losses involving C_{lump} are greatly reduced.

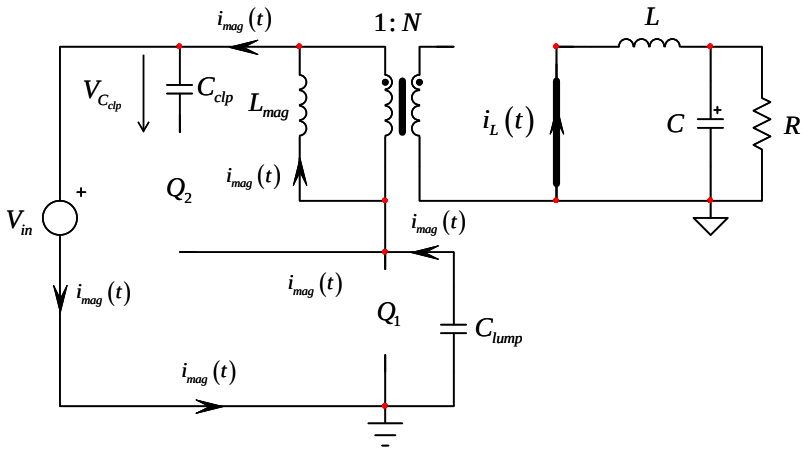

Fig. 7. Q_2 opens slightly before reactivating Q_1 and the magnetizing current now discharges the lumped capacitance.

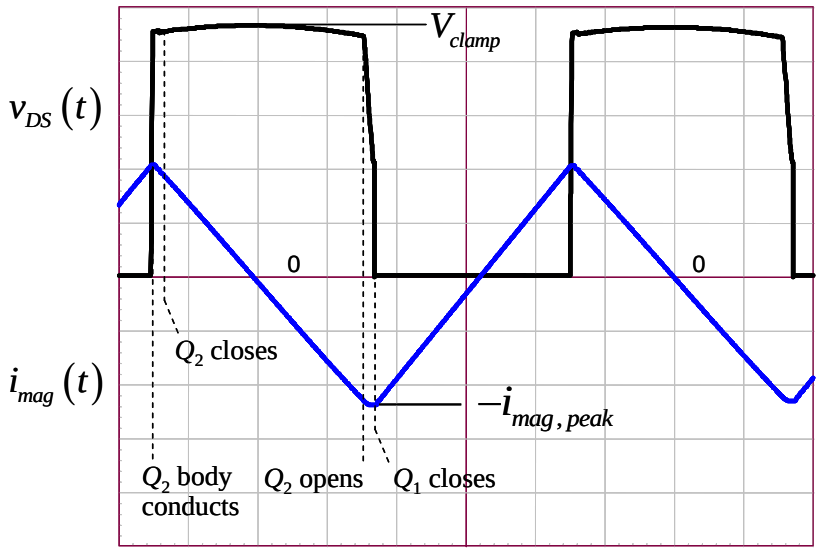

Fig. 8. A delay is inserted prior to turning on the main switch to let C_{lump} discharge.

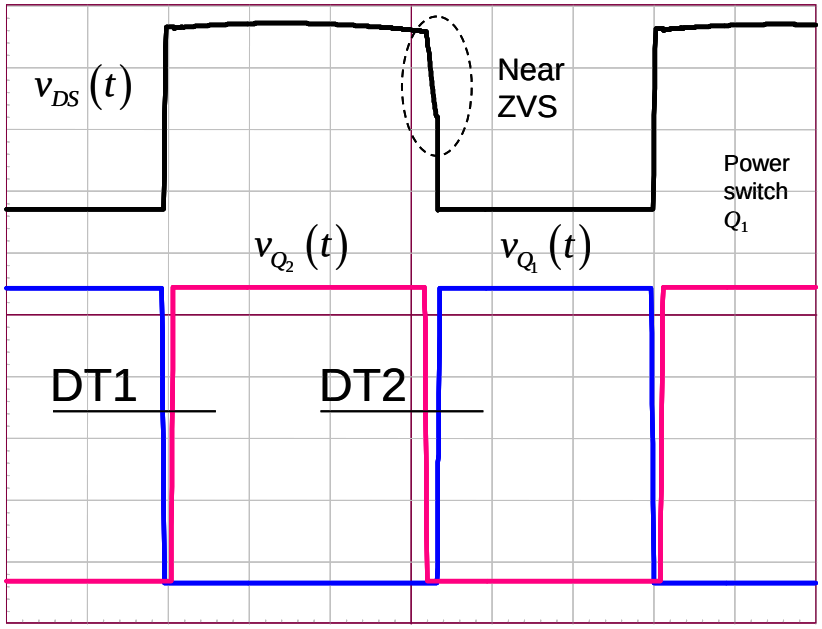

Fig. 9. Dead times are inserted and adjusted to ensure ZVS on the upper-side switch Q_2 but also to give enough time for C_{lump} to discharge prior to reactivating Q_1.

In the active-clamp converter, the magnetizing current is now centered around 0 A, implying a null average value at steady state. Core-wise, the converter now operates the transformer in two quadrants, I and III, while operation was limited to quadrant I with the classical forward structure. This is shown in Fig. 10 where you can see a flux density moving between a negative value (end of off-time) up to a positive value (end of on-time). The core utilization is improved and you can design, if necessary, with a larger flux density swing compared to the classical forward converter.

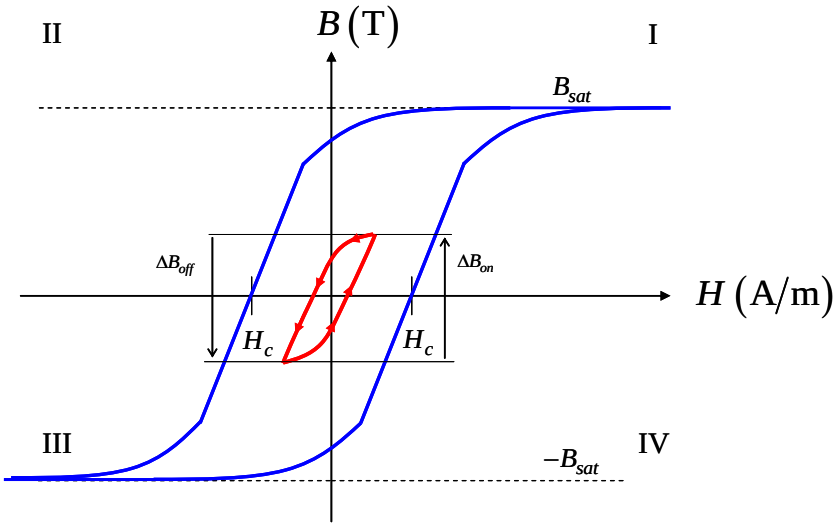

Fig. 10. In the active-clamp configuration, the transformer now operates in two quadrants compared to just one quadrant in the classical forward converter.

Large-Signal Modeling

Large-signal modeling consists of writing the so-called large-signal equations—read "non-linear"—and later linearizing them around an operating point. To apply this technique to the active-clamp converter, we can show [1] that the structure splits into two separate converters:

- the magnetizing current generator, involving the magnetizing inductor, the clamp capacitor and the upper-side series switch Q_2 and
- the isolated buck converter using the primary-side voltage linked to V_{in} and the drop across Q_1, combined with the scaled-down voltage on D_1 anode, further filtered by the *LC* filter before reaching the load.

As explained in reference 1, we can show that these two converters can be treated separately, making the analysis simpler. This is what Fig. 11 shows you. The left side shows the magnetizing current generator, building the magnetizing current in relation to the duty ratio *D*. The right side is the traditional isolated buck representation with the transformer modeled by sources I_2 and V_2.

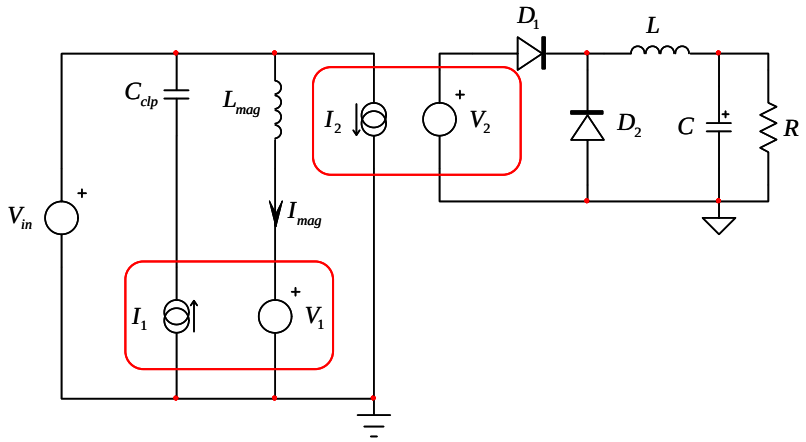

Fig. 11. The active-clamp converter can be modeled as a magnetizing current generator and a classical buck-derived topology.

Small- or large-signal modeling is about waveform averaging, converting a discontinuous time-domain signal into a continuous-time domain equation. If we take the magnetizing current generator, I_1, what do we have? First, the current circulates in the clamp capacitor during the off-time only while, during the on-time, the capacitor sees zero current. We can immediately write the two expressions from which the average value comes:

$$\begin{aligned} i_{clp}(t)\big|_{DT_{sw}} &= 0 \\ i_{clp}(t)\big|_{(1-D)T_{sw}} &= I_{mag} \end{aligned} \rightarrow \left\langle i_{clp}(t) \right\rangle_{T_{sw}} = (1-D) I_{mag} \qquad (9)$$

where I_{mag} is the average magnetizing current.

For the drain voltage source, V_1, the voltage drop across the power switch amounts to what equation 2 describes during the on-time. It then jumps to the clamp voltage during the off-time. Again, we can express the level of the drain voltage during both events and deduce an average value:

$$\begin{aligned} v_{DS}(t)\big|_{DT_{sw}} &= r_{on1}\left(I_{mag}+NI_L\right) \\ v_{DS}(t)\big|_{(1-D)T_{sw}} &= V_{clamp} \end{aligned} \rightarrow \left\langle v_{DS}(t)\right\rangle_{T_{sw}} = V_{clamp}(1-D)+Dr_{on1}\left(I_{mag}+NI_L\right). \quad (10)$$

Fig. 12 shows steady-state waveforms for the drain-source voltage and magnetizing current.

In this expression, V_{clamp} is the voltage at the Q_1 drain node when Q_2 is turned on. It is made of the input voltage plus the clamp capacitor voltage and finally, the voltage drop across Q_2 $r_{DS(on)}$, which is designated r_{on2}:

$$V_{clamp} = V_{in} + V_{clp} + r_{on2}I_{mag}. \quad (11)$$

Please note that I_L in the above expression is the average current flowing through the output inductor L. This current is composed of a small-signal value $\hat{i}_L$ and an average (dc) value, which is I_{out}, the current absorbed by the load.

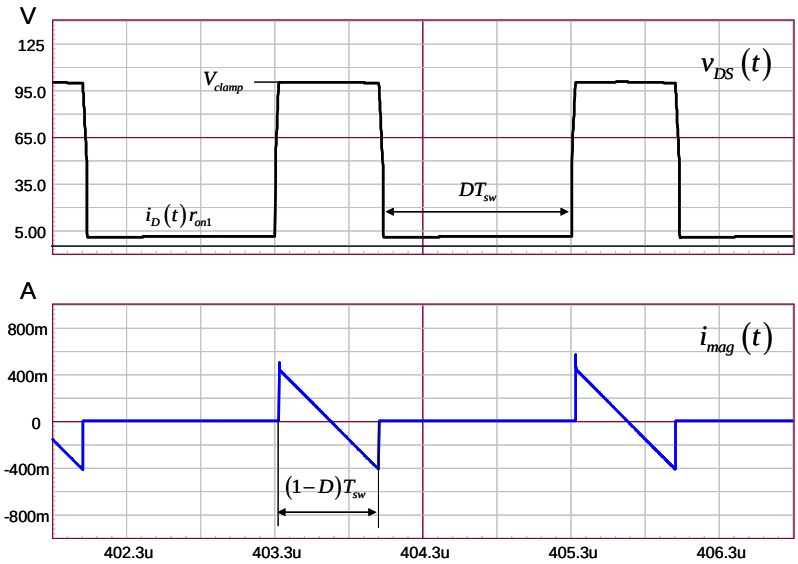

Fig. 12. The drain peaks to the clamp voltage during the off time while the magnetizing current circulates in the clamp capacitor.

The buck stage requires the modeling of the transformer around source I_2 and V_2. The current seen on the transformer primary side $i_p(t)$ is nothing more than the inductor current scaled by the transformer turns ratio N. This current is present when the main switch is turned on, during DT_{sw}. Therefore, we have:

$$\begin{aligned} i_p(t)\big|_{DT_{sw}} &= NI_L \\ i_p(t)\big|_{(1-D)T_{sw}} &= 0 \end{aligned} \rightarrow \left\langle i_p(t)\right\rangle_{T_{sw}} = DNI_L. \quad (12)$$

The secondary-side generator V_2 is actually translating the voltage on the primary side by the transformer turns ratio N. Remember, the primary-side voltage involves the loss across Q_1 when it turns on, as defined by equation 5.

$$\begin{aligned} v_{\sec}(t)\big|_{DT_{sw}} &= N\left(V_{in}-r_{on1}\left(I_{mag}+NI_L\right)\right) \\ v_{\sec}(t)\big|_{(1-D)T_{sw}} &= 0 \end{aligned} \rightarrow \left\langle v_{\sec}(t)\right\rangle_{T_{sw}} = DN\left(V_{in}-r_{on1}\left(I_{mag}+NI_L\right)\right) \quad (13)$$

Once all these sources are associated with a schematic capture, you have the large-signal model of Fig. 13.

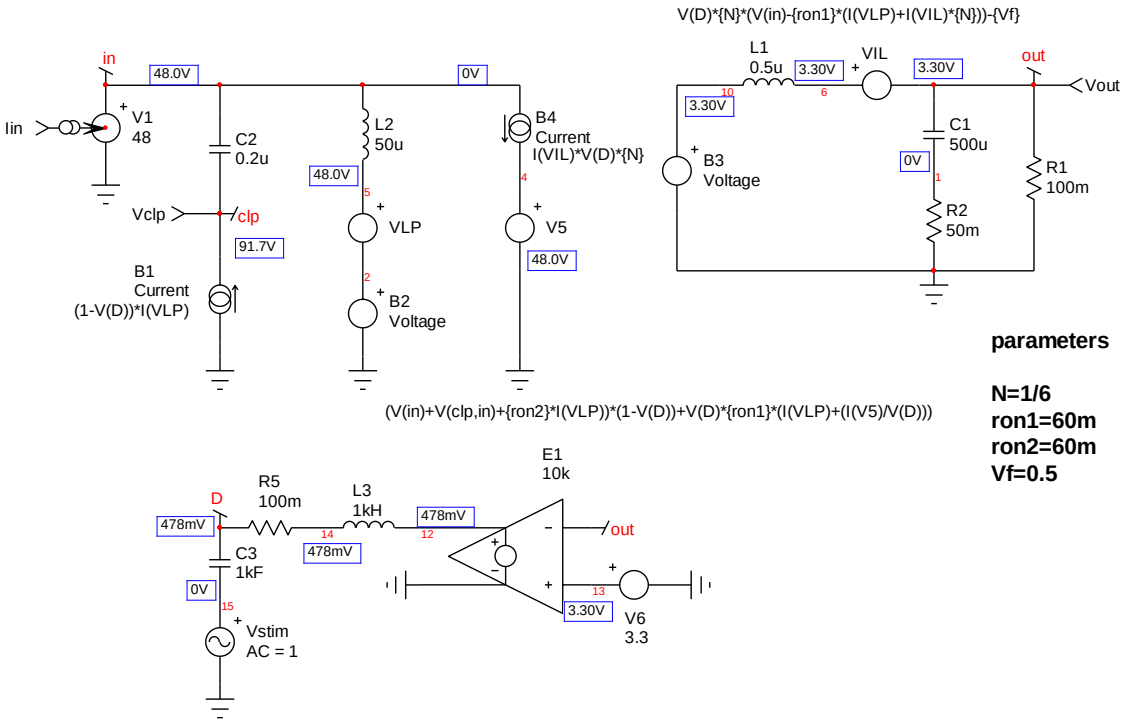

Fig. 13. The large-signal model involves a magnetic current generator and an isolated buck converter.

The voltage-controlled voltage source E_1 provides a dc operating point so that the converter delivers 3.3 V across a 100-mΩ load, R_1. L_3/C_3 classically open the loop in ac but allow the dc bias point calculation to deliver the 3.3-V output level. The model can be used for ac and transient analysis.

What is nice with SPICE is that if you run an ac analysis with a non-linear model, SPICE will first linearize it around a dc operating point and then will ac-sweep it, delivering the Bode plot in a snapshot: you do not need to go through the small-signal study. This is what we are looking for, the control-to-output small-signal response of the active-clamp converter operated in voltage mode. It appears in Fig. 14 and shows the notch incurred by the magnetic current resonance.

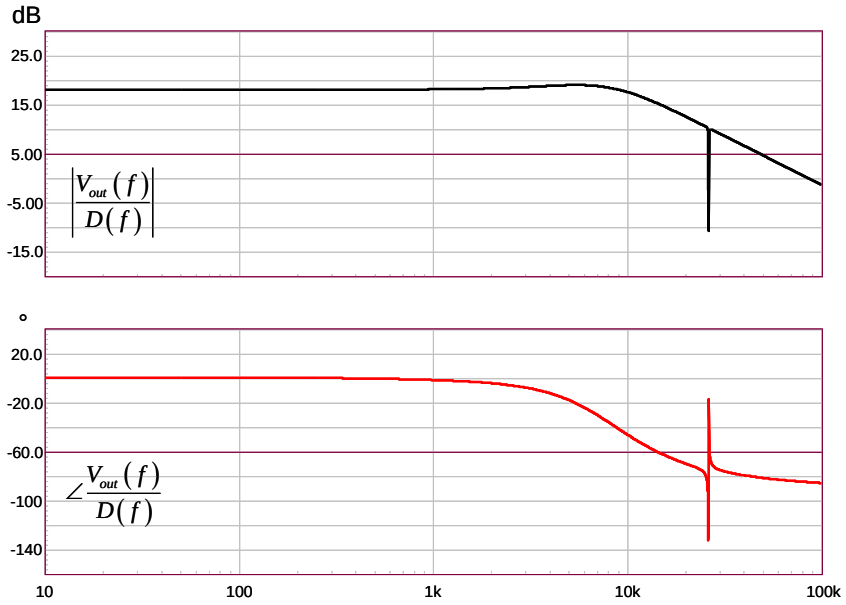

Fig. 14. The large-signal model nicely predicts the presence of the notch in the control-to-output small-signal response of the active-clamp converter operating in voltage mode.

In the next part of this article series, we will see how to derive the complete transfer function of this active-clamp converter operated in voltage mode.

Conclusion

The large-signal active-clamp converter requires a few current and voltage generators which, once properly assembled, lead to a simulation schematic. From this non-linear model, it is possible to quickly obtain a Bode plot as part of an ac simulation. The next and final part of this article series will show how to derive the complete transfer function, backed up with laboratory measurements.

The author wishes to thank Dr. José Capilla from ON Semiconductor for his contribution in developing and testing the large-signal model. Thank you also to Joël Turchi from ON Semiconductor for extensively proof reading the text and equations for this article!

References

1. C. Basso, "Switch Mode Power Supplies: SPICE Simulations and Practical Designs," second edition, McGraw-Hill 2014.
2. D. Dalal, "Design Considerations for the Active Clamp and Reset Technique," TI Application Note SLUP112.
3. J.-C. Pastrana, "Design of 100-W Active Clamp Forward Dc-Dc Converter," AND8273/D, ON Semiconductor.
4. Kurk Mathews, "Design a Simple, Efficient and Reliable Forward Converter," Linear Technology.
5. B.R. Lin and others, "Analysis of an Active Clamp Forward Converter," Power Electronics and Drives Systems, 2005. PEDS 2005,.
6. S. Maniktala, "Active Reset in Forward Converters," Application note, www.microsemi.com.
7. R. Severns, "The History of the Forward Converter," Switching Power Magazine, July 2000.

About The Author

Christophe Basso is an application engineering director at ON Semiconductor in Toulouse, France. He has originated numerous integrated circuits among which the NCP120X series has set new standards for low standby power converters. SPICE simulation is also one of his favorite subjects and he has authored two books on the subject. Christophe's latest work is "Designing Control Loops for Linear and Switching Power Supplies: A Tutorial Guide."

Christophe received a BSEE-equivalent from the Montpellier University, France and an MSEE from the Institut National Polytechnique de Toulouse, France. He holds 30 patents on power conversion and often publishes papers in conferences and trade magazines.

For further reading on the design of forward converters, see the How2Power Design Guide, select the Advanced Search option, go to Search by Design Guide Category and select "Forward" in the Topology category.